

Harmonic Background Amplification in Long Asymmetrical High Voltage Cable Systems

C. F. Jensen

Abstract – This paper presents an analysis of a harmonic problem encountered on the Danish island of Anholt. Time synchronized power quality measurements are presented at transmission and island nodes. Harmonic phase gain factors are calculated from the transmission system to the island and a simulation model is constructed and used to explain the reason for the very high gain factors encountered. A resonance problem is identified and a recommendation is made for the use of phase-domain modelling for long asymmetrical cable systems.

Keywords: Cable modelling, Electromagnetic compatibility, Harmonics, Harmonic amplification, Harmonic propagation, Inter-sequence coupling, Harmonic phase modelling.

I. INTRODUCTION

LONG cable systems at transmission level are becoming more and more common due to public resistance against the installation of new overhead lines (OHLs). The cable systems are used both as a part of the meshed electrical transmission infrastructure and also to form radial connections to single consumers or to production plants such as offshore wind power plants (WPPs). The electrical parameters of high voltage cables are significantly different from those of OHLs. This is especially true of the shunt capacitance, which can be 20–50 times higher on a high voltage cable compared to the equivalent-rated OHL. As a consequence, the system resonances tend to move to lower frequencies, introducing the potential for harmonic background amplification at these frequencies. The combination of the lower-order system harmonic resonances and the harmonic emissions from classical line-commutated hvdc current-source converters has proved to be a challenge in Denmark.

In 2012, the Anholt 400 MW offshore WPP was commissioned. In Denmark, Energinet.dk as the transmission system operator, owns and operates the high voltage cable export system, including the offshore WPP transformers. The Point of Connection (PoC) with the WPP asset owner is at the 33 kV busbars on the low voltage side of the WPP transformers. At the time of commissioning it was noticed that high but manageable levels of 11th- and 13th-order harmonic voltage distortion were present at the PoC of the WPP.

Following a political decision in 2014, Energinet.dk took on

responsibility for the electrical supply to the small Danish island of Anholt, situated off the east coast of Jutland. In order to ensure a cost-effective design, it was decided to connect the new 33 kV cable from the island to the 33 kV side of the Anholt WPP transformers. The geographical location of the Anholt WPP, Anholt island and the high voltage (220 kV) cable connection to the transmission grid can be seen in Fig. 1.

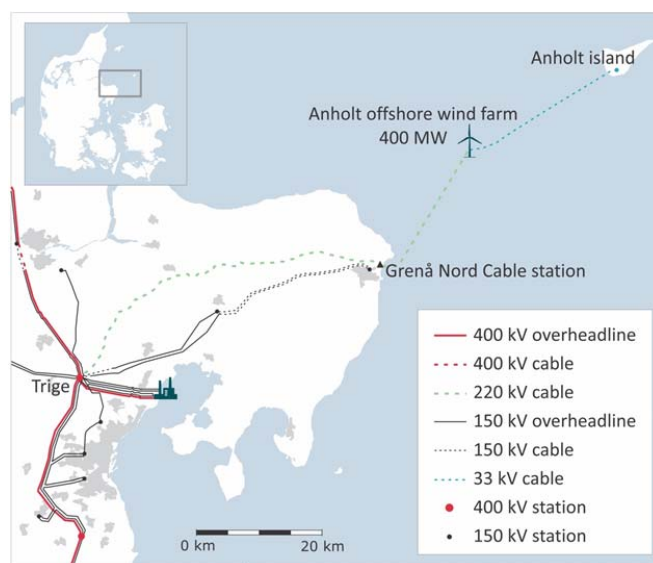


Fig. 1. Geographical location of the Anholt WPP and the island of Anholt.

After the supply to the island was shifted from local generators to mainland supply, the local utility started receiving complaints from consumers on the island. A portable power quality monitoring unit was set up on the island to enable detection and identification of power quality problems related to harmonics.

II. SYSTEM DESCRIPTION

The transmission system connecting Anholt WPP consists of two 400 MVA transformers and three 220 kV cable parts: a 59.6 km cross-bonded land cable laid in flat formation; a 0.5 km beach cable; and a 24.5 km three-core submarine cable. A reactor station (GNK220) is located at the transition point between the land and beach cable. The offshore platform includes three 140 MVA, 220/33 kV transformers. The 33 kV array cable system used to connect the 111 Siemens 3.6 MW wind turbines to the offshore substation has a combined length of 152 km. A single line diagram of the electrical export system and the electrical connection to the island of Anholt is shown in Fig. 2.

Christian Flytkjær Jensen is with the Danish Transmission System Operator Energinet.dk (email of corresponding author: cfj@energinet.dk).

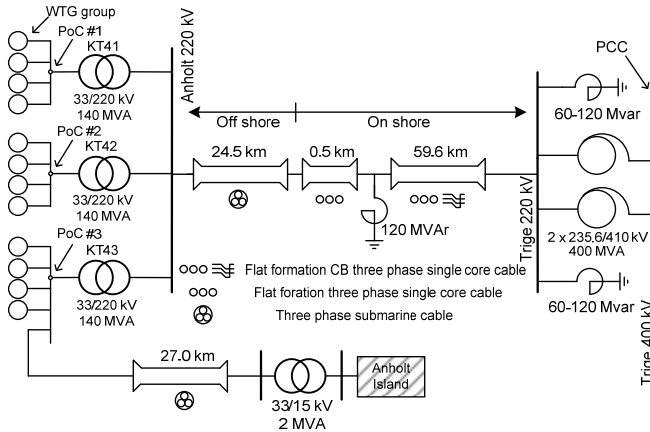


Fig. 2. Electrical export system and the electrical connection to the island of Anholt.

At PoC#3 (see Fig. 2), a 27 km 33 kV cable connects to the island of Anholt. The cable is a three-phase 150 mm² solid conductor aluminium cable with lead alloy sheaths and a common armour. A 33/15 kV 2 MVA transformer supplies the island, with the PoC with the local island utility located at the 15 kV busbars of the island transformer.

The demand on the island is strongly seasonal, varying from 0.2 MW during winter to 1.0 MW during the summer season.

III. POWER QUALITY MEASUREMENT AND ANALYSIS SYSTEM

In order to identify the cause of the problem on the island, accurate high-bandwidth measurements are needed, both at the Trige 400 kV (TRI400) substation and on the island of Anholt (AH0015). Traditional extra high voltage (EHV) instrument transformers are not capable of correctly representing all harmonic frequencies in their secondary circuits due to internal resonance in the measurement systems; this is true of capacitive voltage transformers (CVTs) at all but the fundamental harmonic order, and is true of electromagnetic wound voltage transformers (IVTs) beyond a certain frequency [1]. In recent years, specially designed transducers have been developed that can be retrofitted to traditional CVTs to provide a measuring unit with bandwidth well beyond the 50th harmonic [2]. Using these sensors with CVTs at TRI400, both the magnitudes and phase angles of the harmonics can be determined with good accuracy.

The IVTs at the 15 kV busbars on the island can accurately provide the magnitude of the harmonics in the high voltage signal for frequencies up to around 2000–3000 Hz [1]; no guarantee of accuracy is given for the harmonic phase angles. In this study, only measured harmonic magnitudes up to the 20th harmonic order are discussed and the 15 kV IVTs are therefore suitable for the harmonic measurements.

Statistical harmonic data is obtained using time synchronized commercially available “Class A” power quality meters as defined by IEC 61000-4-7 [3]. All statistical harmonics in this article are expressed as a percentage of the

rms value of the fundamental frequency phase-to-ground voltage and given as 10-minute-aggregated values in accordance with IEC 61000-4-30 [4].

IV. ANALYSIS OF HARMONIC BACKGROUND AMPLIFICATION

In order to identify the cause of the very high harmonic voltage distortion found on the island, the power quality measurements recorded at TRI400 and AH0015 are analysed. The power quality measurements are recorded continuously over a period of 50 weeks. The highest 10-minute-aggregated values over that period are displayed from the 2nd to the 20th harmonic in Fig. 3.

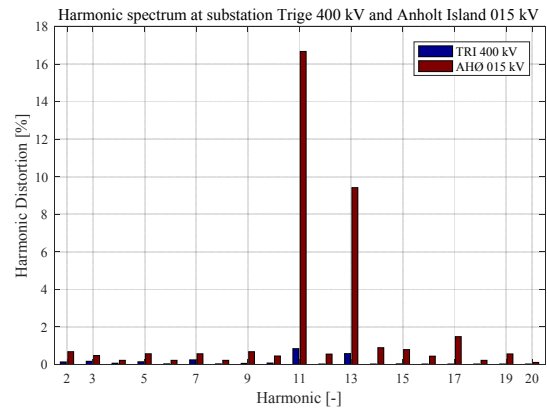


Fig. 3. Highest 10-minute-aggregated harmonic voltages recorded over 50 weeks at TRI400 and AH0015.

The harmonic content at transmission level in Denmark is dominated by the 11th and 13th harmonics, and this pattern is clearly present at Trige in Fig. 3. The highest 11th and 13th harmonic voltages recorded at TRI400 over the 50 weeks are 0.84 % and 0.54 % respectively. These harmonics are, therefore, properly managed. However, at the island, harmonic voltages at the 11th and 13th harmonic orders of 16.7 % and 9.4 % are measured. The time domain voltage at the instance of the highest 11th-order harmonic is displayed in Fig. 4.

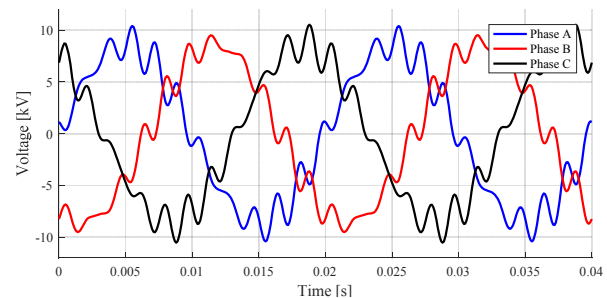


Fig. 4. Time domain voltage signal recorded at AH0015.

The waveforms displayed in Fig. 4 are heavily distorted. This harmonic content is the reason for the complaints received from the island.

In order to investigate the cause of the high harmonic levels on the island, the 11th and 13th harmonics are plotted as functions of time over one representative week in Fig. 5.

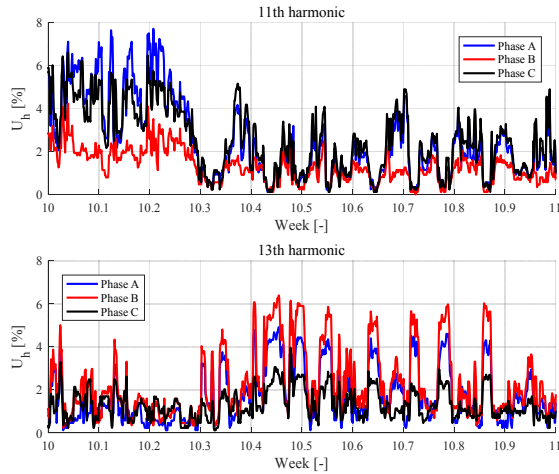


Fig. 5. The 11th- and 13th-order harmonic distortion per phase on the island of Anholt (15 kV) measured over one week.

Fig. 5 gives the first indication of the cause of the problem, as it shows that there is a significant change in the relative levels of the 11th and the 13th harmonic voltages observed before and after week 10.3. This is due to a shift in a system resonance located around the 11th and 13th harmonic. The resonant frequencies shift as the transmission grid harmonic impedance and WPP electrical infrastructure are changed – in turn changing the levels of the 11th- and 13th-order harmonics. Several tests are conducted and active harmonic injection from the wind turbines in the WPP are ruled out as a possible cause of the problem. The cause must, therefore, be background amplification from the transmission system.

In order to further analyse the amplification problem, measured harmonic gains from TRI400 to AH0015 are calculated. For theoretical studies, the sequence-domain harmonic gains (positive, negative and zero sequence) are often used, whereas analysis based on measurements will take phase voltages as the input. The sequence-domain harmonic voltages can be determined at TRI400 due to the transducer type but they cannot be determined at AH0015 since, as mentioned previously, the IVT is not capable of correctly representing the harmonic phase angles. Hence, only the harmonic phase voltage gains are determined. These gains are naturally defined as:

$$G_p(h) = \frac{U_{pY}(h)}{U_{pX}(h)} \quad (1)$$

where $U_{pX}(h)$ and $U_{pY}(h)$ are the harmonic voltages of phase p (A, B, or C) at the h^{th} harmonic at Bus X and Bus Y respectively.

Contrary to the positive-, negative- and zero-sequence harmonic gains, the harmonic voltage gain of one phase is dependent on the flow of harmonics in the other two phases, i.e. the phase equations are coupled. With this in mind, the 11th-order harmonic gain factors per phase from TRI400 to

AH0015 are calculated and plotted in Fig. 6 over one representative day. Fig. 6 (a) shows the three harmonic phase voltages at TRI400 and AH0015 and Fig. 6 (b) shows the resulting gain factors per phase, calculated using (1). (Harmonic voltages at TRI400 below 0.1 % are omitted from the analysis as they can lead to unrealistically high gains due to measurement uncertainties.)

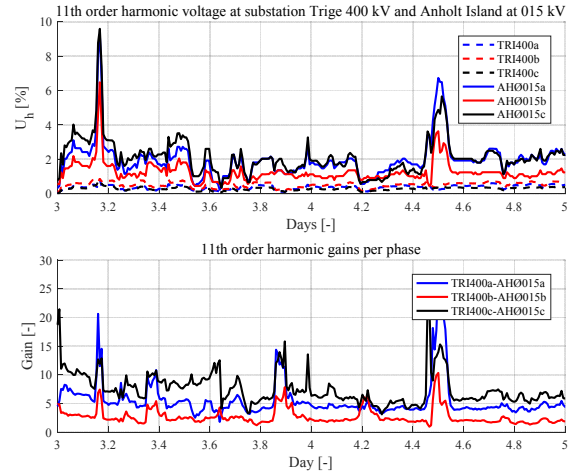


Fig. 6 (a). 11th-order phase-to-ground harmonic voltages at TRI400 and AH0015 and (b), the resulting harmonic gains per phase.

Fig. 6 (b) shows very high gains, typically ranging from 4 to 10. This range of 11th-order harmonic voltage gain was also typical of the whole 50-week measurement period. The cause of the high gains is analysed theoretically in Section VI.

Fig. 7 (a) displays the 13th-order harmonic voltages at TRI400 and AH0015 and (b) shows the resulting 13th harmonic gains over two representative days.

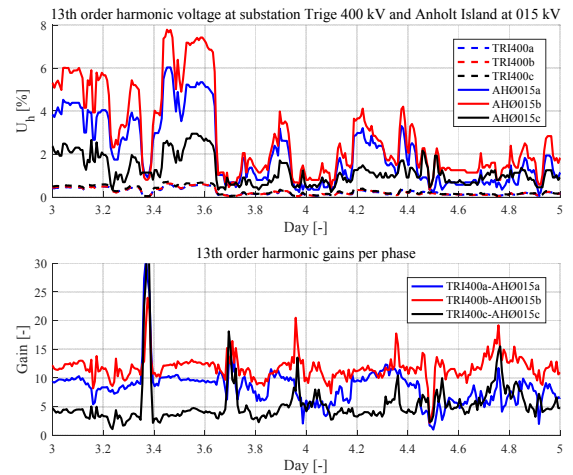


Fig. 7 (a). 13th-order phase-to-ground harmonic voltage at TRI400 and AH0015 and (b), the resulting harmonic gains per phase.

The 13th harmonic phase gains are even higher than the 11th-order gains, ranging from 3.5 to 20. This range of 11th-order harmonic voltage gain was also typical of the whole 50-week measurement period

Both Fig. 6 and Fig. 7 show high harmonic gains from TRI400 to AHØ15. The magnitudes of the gains differ between all three phases for both harmonics. It can be seen that the 13th-order gains are relatively constant over time, compared to the 11th-order gains, whose magnitudes exhibit greater time variation.

V. TRANSMISSION-LEVEL BACKGROUND HARMONIC VOLTAGE DISTORTION

For transmission-level simulation studies and for system design purposes, it is a common approach to either assume that all the harmonic voltages are purely positive sequence or that all non-triplen harmonics are positive sequence and triplen harmonics are zero sequence. However, the field measurements presented from the island of Anholt (Fig. 5, Fig. 6 and Fig. 7) indicate that the harmonic voltages can be significantly unbalanced. For correct harmonic modelling, the background voltage used in a simulation model must represent the true nature of the harmonics at the connecting substation. An unbalanced harmonic voltage can contain a portion of all three sequence components, rendering the aforementioned assumptions invalid.

In Section IV. only harmonics at medium voltage are presented. A typical harmonic spectrum calculated at TRI400 is shown in Fig. 8. The signals used for the analysis are measured using the specially developed high-bandwidth sensors described in Section III. Therefore, both the harmonic magnitudes and phase angles are correctly determined.

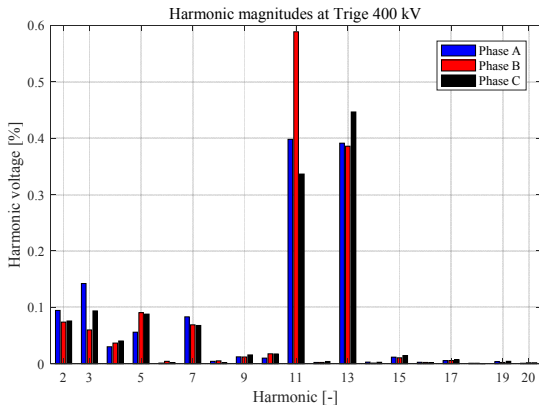


Fig. 8. 400 kV harmonic spectrum at the Trige substation.

With both the harmonic magnitudes and phase angles correctly determined for each phase, the sequence components of the harmonic voltages can be determined using Fortescue's transformation. This is done for the harmonic voltages shown in Fig. 8 and the results are presented in Fig. 9.

The sequence decomposition of the harmonics shows that there is a tendency for most of the harmonics to follow their natural sequences under the balanced system assumption. For instance, the 2nd-order harmonic is predominantly a

negative-sequence harmonic, the 4th is predominantly a positive-sequence harmonic, the 5th is predominantly a negative-sequence harmonic and so on. However, the 11th-order harmonic, that is expected to be negative sequence, contains a significant positive-sequence component (42 % of $U_{2,hl1}$), and the 13th-order harmonic contains a smaller negative-sequence component (10 % of $U_{l,h13}$).

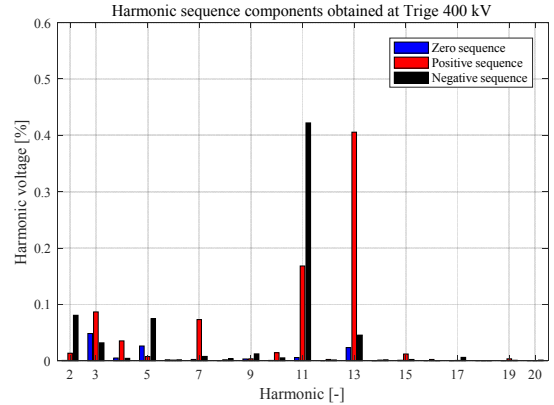


Fig. 9. Harmonic sequence components at Trige 400 kV substation.

Comparing the highest 11th-order harmonic phase voltage in Fig. 8 with the 11th-order negative-sequence harmonic voltage component in Fig. 9, it can be seen that applying the assumption of a single sequence component per harmonic will lead to a significant underestimation of the highest phase-to-ground harmonic voltage (by 42 % in this case).

VI. HARMONIC PROPAGATION ANALYSIS

It is important that the theoretical studies conducted during the planning and design stage can be verified. As shown in Sections V. and VI. assuming that all harmonic voltages are purely positive sequence or that all non-triplen harmonics are positive sequence and triplen harmonics are zero sequence, can lead to significant errors for some harmonics. It is clearly apparent that correctly simulating the unbalanced harmonic voltages on a system like the Anholt cable system requires system models that are based on phase quantities (geometrical input parameters). To investigate this fully, a frequency-dependent phase model of the Anholt cable system and array cable system is constructed in DgSILENT PowerFactory. All cables are modelled based on a geometrical description and all cross bondings are manually implemented. The frequency dependence of the transformers and reactors is included using appropriate multiplication factors [6]. The wind turbines are modelled using a Thévenin equivalent that includes the turbine transformers and the internal filters. The Anholt island system is modelled as a distributed system and the local loads on the island are modelled using the Cigré load model presented in [6]. The detailed model includes the Anholt cable export system up to and including the two 400/220 kV transformers at TRI400. The remainder of the transmission grid is modelled using a Thévenin representation. The Thévenin harmonic impedance is based on impedance polygons, where 300 discrete points, per polygon, per harmonic, are used to

describe the system harmonic impedance. The polygons are constructed using a full-scale harmonic model of the Danish transmission grid.

Using the harmonic simulation model described, the apparent harmonic phase impedance as seen from TRI400 ($Z_p(h) = U_p(h) / I_p(h)$ where p is equal to A, B or C) is presented in Fig. 10 for a fixed harmonic impedance at the Thévenin equivalent at TRI400.

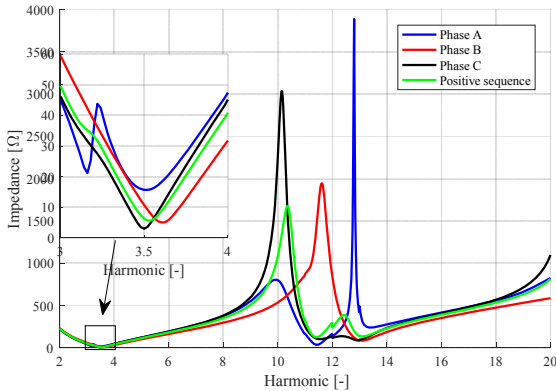


Fig. 10. Phase A, B and C apparent harmonic impedances seen from TRI400.

The impedance–frequency characteristic shows a parallel resonance around the 11th and 13th harmonic order. It can be seen that the resonant frequency of the three phases are different; this would not have been captured using a decoupled sequence-modelling approach.

The theoretical positive-sequence gains from TRI400 to AH0015 for each of the 300 discrete impedance polygon points used to represent the transmission grid seen from TRI400 are presented in Fig. 11.

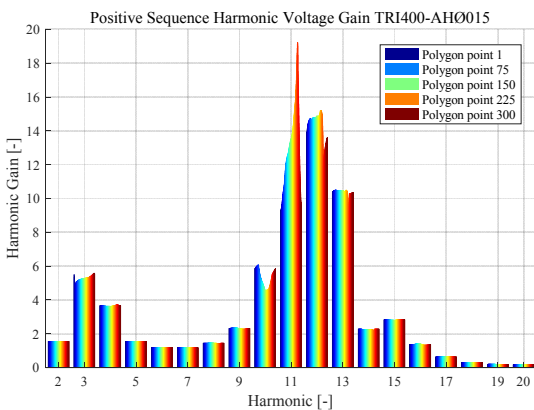


Fig. 11. Positive-sequence gains from TRI400 to AH0015.

The gains indicate that the model has a good fit with the real system behaviour. The magnitudes of the gains fit the measured values (see Fig. 6 and Fig. 7) and Fig. 11 shows that the 11th-order gains are strongly dependent on the harmonic grid impedance, whereas the 13th-order gains do not show this dependence (see Fig. 6 and Fig. 7).

As shown in Fig. 10, the resonant frequencies between the three phases are different. To illustrate the potential error introduced by the default application of the decoupled sequence representation – and hence the positive-sequence gains – the harmonic phase-domain and positive-sequence voltage gains from TRI400 to AH0015 are determined and presented in Fig. 12 for a fixed harmonic impedance at the Thévenin equivalent at TRI400.

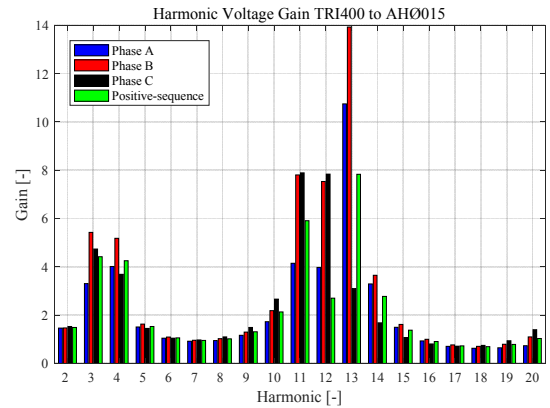


Fig. 12. Harmonic voltage gains from TRI400 to AH0015.

Fig. 12 shows that the phase-domain and the positive-sequence harmonic voltage gains from TRI400 to AH0015 differ significantly in magnitude, with the highest gain always of greater magnitude than the positive-sequence gain. In the case of the 13th harmonic, the highest phase gain is 350 % higher than the lowest phase gain and 79 % higher than the positive-sequence gain. It is clear from a comparison of Fig. 10 and Fig. 12 that the effect is more pronounced at or near to resonant frequencies. The main cause of this behaviour is asymmetrical harmonic propagation on the land cable section from TRI220 to the shunt reactor station. This cable is, as shown in Fig. 2, installed in a flat formation and hence causes mutual inductive coupling that differs between phases. As a result, the harmonic voltages at AH0015 become unbalanced. The gains along the 220 kV and 33 kV submarine cables are equal between phases and also equal to the positive-sequence gain due to the symmetrical formation of the submarine cables (touching trefoil).

The results provided in this section clearly illustrate the need for a harmonic system model based on phase quantities for systems where long cables in flat formation comprise a significant part of the system.

VII. CONCLUSION

This paper discusses the modelling approach for harmonic propagation and assessment studies on systems containing long asymmetrical cable systems. The electrical connection to the Danish island of Anholt is used as a case study.

Time synchronized power quality measurements of the harmonic voltage distortion and resulting high harmonic phase

gains from the Trige 400 kV substation to the 15 kV PoC with the island are presented for the 11th and 13th harmonics. The harmonic gains are very high, ranging from 10 to 20. The measurements also show that the gains per phase are different and as a result, the harmonic voltage distortion on the island is significantly unbalanced.

A harmonic simulation model is developed and the cause of the harmonic problem is found to be a system resonance around the 11th and 13th harmonic leading to high amplification of the existing transmission-level background harmonics. The simulation model also shows that the harmonic gains per phase are expected to be different from each other and different from the positive-sequence gains – this was verified by the measurements. This result is due to the asymmetrical formation of the 59.6 km land cable comprising the first part of the Anholt export cable system. As a consequence, a recommendation for the use of full phase-domain representation for the modelling of long asymmetrical EHV cables is made.

VIII. REFERENCES

- [1] Cigré Technical Brochure 596, "Guideline for Power Quality Monitoring - Measurement Locations, Processing and Presentation of Data," CIGRÉ/CIREC C4.112, 2014.
- [2] F. Ghassemi, P. Gale, T. Cumming and C. Coutts, "Harmonic Voltage Measurements Using CVTs," *IEEE Transaction on Power Delivery* Vol. 20, No. 1, 2005.
- [3] Electromagnetic compatibility (EMC) – Part 4-7: Testing and measurements techniques – General guide on harmonics and interharmonics measurements and instrumentation, for power supply systems and equipment connected thereto, *IEC Standard 61000-3-6, 2008*.
- [4] Electromagnetic compatibility (EMC) – Part 4-30: Testing and measurement techniques – Power Quality measuring methods, *IEC Standard 61000-4-30, 2008*.
- [5] C. F. Jensen, L. H. Kocewiak, Z. Emin, "Amplification of Harmonic Background Distortion in Wind Power Plants with Long High Voltage Connections," Cigré General Session, August 2016.
- [6] Cigré WG CC-02, "Guide for assessing the network harmonic impedance," Cigré Electra 167, July 1996.